C.P. No. 606

C.P. No. 606

MINISTRY OF AVIATION

AERONAUTICAL RESEARCH COUNCIL

CURRENT PAPERS

The Calculated Effect of the Station of Maximum Cross-Sectional Area on the Wave Drag of Delta Wings

by

J. H. B. Smith and W. Thomson

LONDON: HER MAJESTY'S STATIONERY OFFICE

1962

PRICE 4s 6d NET

U.D.C. No. 533.693.3 : 533.692.2 : 533.6.013.12 : 533.6.048.2

C.P. No.606

September, 1961

THE CALCULATED EFFECT OF THE STATION OF MAXIMUM CROSS-SECTIONAL AREA ON THE WAVE DRAG OF DELTA WINGS

by

J. H. B. Smith
and
W. Thomson*

SUMMARY

Use is made of previously calculated properties of a family of delta wings with subsonic leading edges and diamond cross-sections to investigate the effects on the drag and pressure distribution due to volume of variations in the streamwise station at which the cross-sectional area is a maximum. For each station of the maximum cross-sectional area and each value of the aerodynamic slenderness ratio, $\beta s/\ell$, the wing of the family which has least drag for given length and volume is found. As the station of maximum cross-sectional area is moved aft from 65% of the length from the apex, the drag of this optimum wing rises; the rise being steeper for lower values of $\beta s/\ell$. In parallel, adverse pressure gradients and the suction on the wing near the trailing edge both increase so that it becomes less likely that the calculated values will be reproduced in a real flow.

---

*Now of Manchester University. The work was begun while he was a vacation student at the R.A.E. in 1960.

Previously issued as R.A.E. Tech. Note No. Aero 2782 - A.R.C.23,112.

LIST OF CONTENTS

LIST OF APPENDICES

LIST OF TABLES

LIST OF ILLUSTRATIONS

LIST OF ILLUSTRATIONS (CONTD)

1 INTRODUCTION

One approach to the design of a large transport aircraft is to accommodate the fuel and as much as possible of the payload within the wing. For supersonic flight this leads to a search for sharp-edged delta-like wings with subsonic leading edges which have low wave drag due to volume. Although other considerations make it likely that the planform of such an aircraft would have streamwise tips and that its cross-sections would bulge along the centre-line, relative ease of calculation leads us to make preliminary investigations on delta wings with diamond cross-sections.

Such wings have been studied by various fully and partially linearized theories appropriate to subsonic, transonic and supersonic speeds in an extensive series of R.A.E. papers. A number of them have also been tested in wind tunnels and in free-flight. One result of this work has been to establish that two particular wings, the "Newby" and the "Lord V", have low drag for given volume and length over a range of the aerodynamic slenderness parameter $\beta s/\ell$ ($\beta^2 = M^2-1$, s = semi-span, ℓ = length). These wings are completely defined by their centre-sections which can be described by the equations:

$$\text{"Newby"} \qquad z(\xi,0) = \pm \frac{V}{2s\ell}\, 12\xi(1-\xi) \tag{1}$$

$$\text{"Lord V"} \qquad z(\xi,0) = \pm \frac{V}{2s\ell}\, 7\xi(1-\xi)(4-6\xi+4\xi^2-\xi^3) \tag{2}$$

where the origin is at the wing apex, the x-axis is along the centre-line of the wing, the z-axis is normal to the wing plane and $\xi = x/\ell$. These centre-sections are illustrated in Fig.1, with the corresponding cross-sectional area distributions in Fig.2.

A convenient standard of comparison for the volume-dependent drag of slender configurations is the drag of the optimum slender pointed body of revolution of given length and volume (the Sears-Haack body):

$$\frac{D}{q} = \frac{128}{\pi}\,\frac{V^2}{\ell^4}\,. \tag{3}$$

We shall use K_o, the ratio of the drag of a wing to the drag of the Sears-Haack body of the same length and volume, as a measure of drag. Fig.3 shows values of K_o for the "Newby" and "Lord V" wings. It is clear that there is a difference of 10-15% between the values calculated by thin-wing theory* and those derived by the integration of measured pressure

---

*We shall use "thin-wing theory" to mean the theory of inviscid irrotational flow based on the linearized potential equation, in which boundary conditions satisfied on the wing surface are applied in the plane of the wing and flow variables required on the wing surface are evaluated in the plane of wing. The pressure is obtained from the linearized Bernoulli equation. The further qualification in "slender thin-wing theory" will imply that the assumption of slenderness ($|\beta^2\phi_{xx}| \ll |\phi_{yy}| + |\phi_{zz}|$) has been made in addition.

distributions. On the other hand, the differences between the drags of the two wings and the trends of the drags with Mach number are both well represented by the theory.

We have said that these two wings have low drag and have displayed the relevant values of K_o, but it is not easy to make the statement more precise. Even if we confine our attention to thin-wing theory, making all the assumptions implied therein, we do not know the minimum drag of a wing with given planform and volume. However, if we are prepared to limit ourselves to delta wings with diamond cross-sections whose centre-sections are polynomials of degree five, the curve labelled "unrestricted optimum" of Fig.4 can be obtained from the results of Ref.1. For $0.2 \leq \beta s/\ell \leq 0.8$, one or other of the two wings ("Newby" and "Lord V") has a value of K_o which is within 10% of the optimum. In view of the uncertainties of the theory, we may doubt the value of an attempt to use it to find wings of this family with lower values of K_o.

The designer, however, is as concerned with how the volume is distributed over the planform as with the volume itself, so we should consider restrictions on the distribution of volume. For a slender wing the constraints on the volume distribution which can be expected to have most effect on the drag are those imposed on the cross-sectional area distribution. We consider the simplest of these: we fix the lengthwise station at which the cross-sectional area distribution has its maximum value*.

2 RESULTS

The "Lord V" wing has an area distribution with its peak at 55% of its length from the apex. Fig.4 shows how its drag varies compared with the optimum curve for wings of the present family which have their maximum cross-sectional areas at the same station. The theoretically possible improvement never exceeds 4%. The cross-sectional area distribution of the "Newby" wing has a maximum at 2/3 of its length; its drag is shown in Fig.4 compared with the corresponding minimum curve. At $\beta s/\ell = 0.4$, there is now apparently 15% to be gained.

The general picture of the variation in minimum drag with $\beta s/\ell$ when the station of maximum cross-sectional area is fixed is shown in Fig.5. The usual tendency for K_o to decrease as $\beta s/\ell$ increases is seen to be most pronounced when the maximum cross-sectional area occurs aft. When it is far enough forward the decrease in K_o as $\beta s/\ell$ increases through small values is reversed at the larger values. Although for $0.3 \leq \beta s/\ell \leq 0.7$ a wing with its maximum cross-sectional area near 60% of its length is best, the proximity of the curves for 50% and 70% suggest that the optimum is flat. The same values are shown in Fig.6 in a plot of K_o against station of maximum cross-sectional area for fixed $\beta s/\ell$. These show how the best position for the largest cross-section moves back from 50% at $\beta s/\ell = 0$ to 67% at $\beta s/\ell = 0.8$. They also show a rapid and substantial increase in K_o at low values of $\beta s/\ell$ as the maximum cross-section is moved aft. However, there is a fair-sized region of the diagram where K_o is no more than 0.8 and the maximum cross-section is not less than 65% of the length from the apex.

---

*More precisely, we make $S'(\bar{\xi}) = 0$. See Appendix 1 for details.

Since tentative layouts of supersonic transports indicate that the maximum cross-sectional area should be considerably further aft than the 55% of the "Lord V", we shall look at some of the wings in this region in more detail. Each of the eight points lettered A-H on Fig.6 corresponds to a wing which, at its design value of $\beta s/\ell$, has the least drag of any wing in the family we have considered with its maximum cross-sectional area at the same station. The values of K_o are all less than 0.8. There are three wings H,E,A with $\bar{\xi} = 0.65$ designed for $\beta s/\ell = 0.4$, 0.6 and 0.8, two wings F,B with $\bar{\xi} = 0.70$ designed for $\beta s/\ell = 0.6$ and 0.8, two wings G,C with $\bar{\xi} = 0.75$ designed for $\beta s/\ell = 0.6$ and 0.8 and wing D with $\bar{\xi} = 0.8$ designed for $\beta s/\ell = 0.8$. The variation in drag of these wings at other values of $\beta s/\ell$ is displayed in Fig.7. We see that a change in $\bar{\xi}$ of 0.05 affects the drag at a given $\beta s/\ell$ more than a change of 0.2 in the $\beta s/\ell$ for which the wing was designed. In particular, the advantage of H over E is so slight that we consider it no further*, thus limiting our attention to two design values of $\beta s/\ell$.

The centre-sections of the wings A-G are illustrated in Figs.8 and 9, with the corresponding cross-sectional area distributions in Figs.10 and 11. The wings which have $\bar{\xi} = 0.75$ and 0.8 (C,G,D) have points of inflexion in their centre-sections. The 'dip' becomes larger for the lower design value of $\beta s/\ell$ and for the further aft $\bar{\xi}$. In the case of wing D, the 'dip' persists in the area distribution. Some of these dips may be introduced by the search for an optimum within a restricted family of shapes. In this case we should expect there to be wings outside the family without the dips and with lower drags. It is of some interest that the first 20% of the wing has a shape decided primarily by the choice of $\beta s/\ell$ and the last 20% is decided primarily by the choice of $\bar{\xi}$, as Fig.10 shows clearly. We do not find any evidence that the drag is related to the maximum cross-sectional area, except for wings which have their maximum areas at the same station.

The predictions of inviscid flow theory are liable to be invalidated by the occurrence of boundary layer separation forward of the trailing-edge, either ordinary or shock-induced. The possibility of ordinary separation from the wing surface is avoided by a pressure field over the wing in which the pressure falls monotonically both in the stream direction and inwards from the leading edge to the centre-line, as is shown in Ref.2. The same pressure field avoids the possibility of shock-waves occurring on the wing in properly supersonic** inviscid flow. However, if the pressure at the trailing-edge is below that at infinity, the recompression behind the wing may take place through a shock system and if it does so in viscous flow there may be a forward branch of the system on the wing surface with a separated boundary layer behind it. Without a deeper investigation of the flow near the trailing-edge we can only be sure of avoiding this separation by requiring that the pressure coefficient remains positive at the trailing-edge. In fact it may not be possible to find a wing which has favourable pressure gradients and a positive trailing-edge pressure coefficient. Fortunately there are many cases in which one or more of these conditions is violated and the real flow still approximates to the inviscid flow model; the various rises in pressure being small enough and slow enough for a thin boundary layer or wake to accommodate itself. However, we should be cautious

*As we should expect, H and E are almost the same shape.

**At low supersonic Mach numbers it seems to be possible for a normal shock to occur near the trailing-edge of a delta wing in inviscid flow. If the trailing-edge angle on the centre-line exceeds twice the maximum deflection angle possible through an oblique shock at the local Mach number of the flow there, then it is likely that a normal shock will occur on the centre-line upstream of the trailing-edge, on the analogy of the flow over a wedge where the bow shock is detached. There seems to be no reason why this should not be associated with a pressure distribution, as calculated by thin-wing theory, which is favourable in the sense described above.

in accepting the pressure drag estimates of inviscid theory when these are associated with rapid increases in pressure in the stream direction or with large suctions near the trailing-edge. Of course, failure to realise the attached flow over the rear of such a wing could result in a pressure drag which was lower rather than higher than the theoretical estimate. However, this drag would depend on Reynolds number, and, more seriously, the associated flow would be sensitive to trailing-edge conditions. At best the forward branch of the trailing-edge shock system could be expected to move across the rear of the wing as, for instance, elevon settings were altered. At worst the flow might be unsteady. The pressure distributions on wings A-G have been investigated with the above considerations in mind.

Although the drag of the "Newby" wing changes rapidly with $\beta s/\ell$ (Fig.4), the character of the pressure distribution near the centre-line shown in Fig.12 (extracted from Ref.3) is little affected. We have therefore not considered the pressure distributions at a range of values of $\beta s/\ell$ for all the wings. Fig.13 shows the pressure distribution on a "Lord V" wing (again from Ref.3) at various spanwise stations at one value of $\beta s/\ell$. The character of the pressure distribution is well represented by the variation at two spanwise stations*, $y/s = 0.05$ and $y/s = 0.575$, so we show the distribution on wings A-G at these stations only.

The wings A-D whose pressure distributions at $\beta s/\ell = 0.8$ are shown in Fig.14(a)-(d) are all designed for $\beta s/\ell = 0.8$ and for values of $\bar{\xi}$ of 0.65, 0.7, 0.75 and 0.8 respectively. Both thin-wing theory and slender thin-wing theory values have been calculated as described in Appendix 2, but our discussion is in terms of the thin-wing theory values only. Wing A has a wholly favourable pressure field, falling from front to rear and from leading edge to centre-line. Its trailing-edge suction is less than that of the "Newby" wing. Its calculated drag is a little below that of the "Newby" wing at $\beta s/\ell = 0.8$; at $\beta s/\ell = 0.4$ its calculated drag is well below that of the "Newby" wing and actually below the measured drag of the latter.

Wing B shows an insignificant adverse streamwise pressure gradient and a little more suction near the trailing-edge than wing A. Wing C has a slight adverse streamwise gradient and a marked increase in trailing-edge suction. Wing D has a definite adverse streamwise gradient, a slight adverse gradient from leading edge to centre-line near $\xi = 0.75$ and a large trailing-edge suction. Moving the station of maximum cross-sectional area aft from 0.65 to 0.8 therefore not only increases K_o from 0.65 to 0.8, as shown in Fig.6, but also reduces the likelihood of realizing the assumed type of flow.

Referring now to Figs.14(e) - (g), we see that the pressure distributions on wings E,F and G designed for $\beta s/\ell = 0.6$ and $\bar{\xi} = 0.65$, 0.7 and 0.75 respectively show the same trends as those on wings A-D. If we consider two wings with the same value of $\bar{\xi}$ optimized for different values of $\beta s/\ell$ and compare the pressure distributions at the design values of $\beta s/\ell$, we find that the unfavourable features are more severe for the lower value of $\beta s/\ell$. To determine whether this is due to the change in $\beta s/\ell$ at which the pressures are calculated or the change in design $\beta s/\ell$, we show additionally on Fig.14(g) the pressure distribution on wing G at $\beta s/\ell = 0.8$, the design value for wings A-D. Both the adverse gradient and the trailing-edge suction are reduced at the higher $\beta s/\ell$. Comparing wings C and G ($\bar{\xi} = 0.75$ for both) at $\beta s/\ell = 0.8$, we see that G has a steeper adverse gradient but less trailing-edge

*The numerical values of y/s are chosen to take advantage of Eminton's work[3]. They, and the values of $\beta s/\ell$, are related to tests of particular wings.

suction. However, all these differences between the pressure distributions on wings with the same ξ are relatively small. It is doubtful whether they have any relevance outside the present theory or even outside the present family of wings.

Finally, for completeness, the drags of wings A-H have been evaluated by slender-body theory. The results are shown in Fig.15. One can conclude that slender-body theory becomes less appropriate as the station of maximum cross-sectional area is moved aft, as would have been expected from the pressure distributions of Fig.14.

CONCLUSIONS

Area distributions for delta wings with diamond cross-sections have been found in which the maximum cross-sectional area occurs towards the rear of the wing and the calculated drag due to volume is low, at least at the higher values of $\beta s/\ell$. When the station of maximum cross-sectional area is aft of 65% of the length from the apex, the drag increases as it moves further aft for all values of $\beta s/\ell \leq 0.8$. When the maximum cross-sectional area occurs at any fixed station aft of 60%, the wings designed for the higher values of $\beta s/\ell$ have lower drag than those designed for lower values of $\beta s/\ell$ at their respective design points.

Because of the predicted occurrence of unfavourable pressure fields and large trailing-edge suctions, the postulated type of flow becomes less likely to occur on the wings where the maximum cross-sectional area is further aft, owing to possible boundary layer separations.

LIST OF SYMBOLS

A_i $(0 \leq i \leq 3)$ coefficients which determine the shape of the wing

C_p pressure coefficient

C_{p_i} $(1 \leq i \leq 4)$ pressure coefficient on four basic wings

D drag

D_i $(0 \leq i \leq 9)$ drags of ten basic wings

K_o $(\pi\ell^4/128V^2)(D/q)$ volume-dependent drag factor

ℓ length

M Mach number

q kinetic pressure

s semi-span

$S(\xi)$ cross-sectional area

V volume

x,y,z right-handed Cartesian coordinates, origin at wing apex, Ox along wing centre-line and Oy to starboard in the wing plane

LIST OF SYMBOLS (CONTD)

β	$(M^2-1)^{\frac{1}{2}}$
ξ	x/ℓ
$\bar{\xi}$	value of ξ at which $S'(\xi) = 0$
ϕ	disturbance velocity potential

LIST OF REFERENCES

No.	Author	Title, etc.
1	Weber, J.	Some notes on the zero-lift wave drag of slender wings with unswept trailing-edges. A.R.C. R. & M.3222. December, 1959.
2	Maskell, E.C. Weber, J.	On the aerodynamic design of slender wings. J.R. Aero. Soc. Vol.63, p.709. December, 1959.
3	Eminton, E.	Pressure distribution at zero-lift for delta wings with rhombic cross-sections. A.R.C. C.P. No.525. October, 1959.
4	Weber, J.	Slender delta wings with sharp edges at zero lift. A.R.C.19549. May, 1957.

APPENDIX 1

CALCULATION AND MINIMIZATION OF THE DRAG DUE TO VOLUME

With the origin at the wing apex, Ox along the centre-line, Oy to starboard in the plane of the wing and Oz completing the right-handed system, the equation to the starboard upper surface of the delta wing which we consider is:

$$z(x,y) = \frac{\ell^2}{2s}(\xi - y/s)(1 - \xi) \sum_{n=0}^{3} A_n \xi^n \qquad (4)$$

where s is the semi-span, ℓ is the length and $\xi = x/\ell$. The thickness vanishes along the leading edge $y = s\xi$. z is a linear function of y, so the cross-sections are rhombic. The centre-section is given by the quintic polynomial:

$$z(x,o) = \frac{\ell^2}{2s}\xi(1 - \xi) \sum_{n=0}^{3} A_n \xi^n . \qquad (5)$$

The cross-sectional area, $S(\xi)$, is given by

$$S(\xi) = 4\int_{o}^{s\xi} z(x,y)dy = \ell^2 \xi^2(1 - \xi) \sum_{n=0}^{3} A_n \xi^n \qquad (6)$$

and the volume, V, by

$$V = \int_{o}^{\ell} S(\xi)dx = \ell^3 \sum_{n=0}^{3} \frac{A_n}{(n+3)(n+4)} . \qquad (7)$$

According to thin-wing theory, the drag of a wing of this family is clearly a quadratic form in the coefficients A_n. In Ref.1 (Table 2*) the values of $D/q\ell^2$ for ten independent wings of the family are quoted for $\beta s/\ell = 0.2(0.1)0.8$. This Table is reproduced as Table 1 of the present paper. If the drags of the wings of this Table are denoted by D_o, D_1, ... D_9, the drag of the general member of the family (4) is

---

*The algebra would be a little simpler if we used the presentation of Table 3 of Ref.1. However, the values quoted there have been rounded off and the slight loss of significance would upset the sensitive minimization procedure.

$$D = (A_0 + A_1 + A_2 + A_3)(D_0A_0 + D_1A_1 + D_2A_2 + D_3A_3) - D_4A_0A_1$$

$$- D_5A_0A_2 - D_6A_0A_3 - D_7A_1A_2 - D_8A_1A_3 - D_9A_2A_3 \,. \qquad (8)$$

The condition that the wing has its maximum cross-sectional area at a particular lengthwise station $\xi = \bar{\xi}$ is not easily formulated. We replace it by the condition that the cross-sectional area $S(\xi)$ has a local extremum at $\xi = \bar{\xi}$ i.e.

$$S'(\bar{\xi}) = \ell^2 \sum_{n=0}^{3} A_n \left((n+2)\bar{\xi}^{n+1} - (n+3)\bar{\xi}^{n+2} \right) = 0. \qquad (9)$$

The results produced can then be inspected to determine that the extremum is a maximum and that this is the greatest local maximum.

To find the wing of the family which has the least drag for a given volume of, say, ℓ^3 and given $\bar{\xi}$, we have simply to solve the six simultaneous equations:

$$\left.\begin{aligned} \frac{\partial}{\partial A_n}\left(\frac{D}{q\ell^2} + \lambda\left(\frac{V}{\ell^3} - 1\right) + \mu\,\frac{S'(\bar{\xi})}{\ell^2}\right) &= 0 \qquad n = 0,1,2,3 \\ \frac{V}{\ell^3} - 1 &= 0 \\ S'(\bar{\xi}) &= 0 \end{aligned}\right\} \qquad (10)$$

for the coefficients A_n and the Lagrangian multipliers λ and μ, where D/q is given in terms of the A_n by equation (8), V by equation (7) and $S'(\bar{\xi})$ by equation (9). We then know the shape of the wing by equation (4) and its drag by equation (8).

This has been done for $\beta s/\ell = 0.2(0.1)0.8$ and a range of values of $\bar{\xi}$. The resulting values of $K_o = \frac{\pi\ell^4}{128V^2}\,\frac{D}{q}$ have been plotted in the figures.

For the particular wings A-H of Fig.6, the coefficients A_n are tabulated in Table 2. The shapes of these wings, plotted in Figs.8-11, show that the local extremum at $\bar{\xi}$ is the only maximum of the cross-sectional area distributions. However, a check on the area distribution of the wing corresponding to $\bar{\xi} = 0.85$ and $\beta s/\ell = 0.8$ in Fig.6 showed that this has two maxima; the rearward one at $\bar{\xi} = 0.85$ is slightly lower than the forward one. No other checks have been carried out, but it is to be expected that many of the wings corresponding to high values of $\bar{\xi}$ and low values of $\beta s/\ell$ will have more than one local maximum.

The drag of the wings A-H is readily calculated by thin-wing theory using equation (8) and Table 1. The drag has also been calculated according to slender-body theory. (Slender-body theory and slender thin-wing theory are equivalent so far as the drag of wings with straight unswept trailing-edges is concerned.) The formula appropriate to this family of wings has been given by Weber[1]. It is

$$K_o = \frac{1}{256}\left\{ -\frac{5}{4}A_0^2 - \frac{23}{12}A_1^2 - \frac{55}{24}A_2^2 - \frac{307}{120}A_3^2 - \frac{7}{2}A_0A_1 - \frac{13}{3}A_0A_2 \right.$$

$$- 5A_0A_3 - \frac{13}{3}A_1A_2 - \frac{29}{6}A_1A_3 - \frac{59}{12}A_2A_3$$

$$\left. + (A_0 + A_1 + A_2 + A_3)^2 \left[k - \ell n \frac{\beta s}{\ell} \right] \right\} \qquad (11)$$

where $k = \frac{25}{12} - \frac{1}{3}\ell n 2$ is the value appropriate to rhombic cross-sections.

APPENDIX 2

CALCULATION OF PRESSURE DUE TO VOLUME

Eminton has programmed the calculation, according to thin-wing theory, of the pressure due to volume on wings of the present family. In Ref.3 she tabulates the chordwise pressure distribution at two spanwise stations on four basic volume distributions for two values of $\beta s/\ell$. For the present work, she has calculated these for a further value of $\beta s/\ell$ and the complete tabulation is reproduced here as Table 3. The choice of the spanwise stations and the two lower values of $\beta s/\ell$ was originally to conform with experimental configurations.

For the general wing of the family, equation (4), the pressure coefficient is given in terms of the C_{p_i} $(i = 1,2,3,4)$ of Table 3 by

$$C_p = \sum_{n=1}^{4} A_{i-1} C_{p_i} . \qquad (12)$$

The pressure coefficient has also been calculated by slender thin-wing theory, by equation (50) of Ref.4. The expression is not reproduced here on account of its length.

TABLE 1

Values of $D/q\ell^2$ for ten basic wings of the family (thin-wing theory)

Coefficients				$\beta s/\ell$						
A_0	A_1	A_2	A_3	0.2	0.3	0.4	0.5	0.6	0.7	0.8
1	0	0	0	0.3601	0.3032	0.2658	0.2391	0.2190	0.2039	0.1928
0	1	0	0	0.2587	0.2050	0.1701	0.1452	0.1266	0.1122	0.1007
0	0	1	0	0.2053	0.1560	0.1250	0.1037	0.0882	0.0765	0.0673
0	0	0	1	0.1703	0.1251	0.0978	0.0797	0.0669	0.0575	0.0503
1	-1	0	0	0.0506	0.0491	0.0478	0.0467	0.0459	0.0455	0.0456
1	0	-1	0	0.1168	0.1110	0.1057	0.1013	0.0977	0.0948	0.0930
1	0	0	-1	0.1705	0.1594	0.1495	0.1410	0.1339	0.1282	0.1242
0	1	-1	0	0.01764	0.01627	0.01498	0.01382	0.01281	0.01191	0.01110
0	1	0	-1	0.0488	0.0441	0.0399	0.0362	0.0329	0.0301	0.0277
0	0	1	-1	0.00869	0.00764	0.00672	0.00592	0.00525	0.00470	0.00424

TABLE 2

Coefficients of lowest drag wings of the family for unit V/ℓ^2

reference letter	design $\beta s/\ell$	design $\bar{\xi}$	coefficients				K_o at design (thin-wing theory)
			A_0	A_1	A_2	A_3	
A	0.8	0.65	24.90	-52.20	67.44	-29.93	0.646
B	0.8	0.70	27.15	-72.48	103.14	-45.22	0.651
C	0.8	0.75	26.65	-62.52	66.04	-12.44	0.698
D	0.8	0.80	22.53	-20.87	-34.58	55.39	0.779
E	0.6	0.65	33.30	-91.32	125.75	-58.83	0.679
F	0.6	0.70	35.45	-107.97	151.16	-66.97	0.706
G	0.6	0.75	31.95	-77.43	74.86	-12.04	0.775
H	0.4	0.65	35.37	-99.11	133.57	-60.66	0.789

TABLE 3

Pressure coefficients for four basic wings of the family (thin-wing theory)

$\beta s/\ell = 0.416$

y/s	ξ	C_{p_1}	C_{p_2}	C_{p_3}	C_{p_4}
0.05	0.1	0.901	0.218	0.035	0.005
	0.2	0.560	0.351	0.125	0.037
	0.3	0.282	0.392	0.228	0.105
	0.4	0.012	0.341	0.303	0.196
	0.5	-0.255	0.198	0.311	0.275
	0.6	-0.522	-0.035	0.211	0.289
	0.7	-0.788	-0.359	-0.035	0.160
	0.8	-1.054	-0.774	-0.469	-0.209
	0.9	-1.319	-1.280	-1.128	-0.937
	1.0	-1.585	-1.876	-2.053	-2.163
0.575	0.6	0.284	0.463	0.393	0.279
	0.7	-0.321	0.106	0.257	0.278
	0.8	-0.711	-0.280	-0.020	0.120
	0.9	-1.047	-0.753	-0.509	-0.324
	1.0	-1.360	-1.320	-1.252	-1.188

$\beta s/\ell = 0.577$

y/s	ξ	C_{p_1}	C_{p_2}	C_{p_3}	C_{p_4}
0.05	0.1	0.778	0.178	0.027	0.004
	0.2	0.484	0.291	0.101	0.029
	0.3	0.253	0.328	0.185	0.083
	0.4	0.031	0.290	0.249	0.157
	0.5	-0.188	0.180	0.260	0.223
	0.6	-0.407	-0.004	0.187	0.240
	0.7	-0.625	-0.260	-0.001	0.147
	0.8	-0.842	-0.590	-0.336	-0.131
	0.9	-1.060	-0.993	-0.849	-0.686
	1.0	-1.278	-1.469	-1.571	-1.628
0.575	0.6	0.443	0.464	0.331	0.213
	0.7	-0.144	0.169	0.238	0.223
	0.8	-0.493	-0.132	0.045	0.124
	0.9	-0.785	-0.503	-0.311	-0.184
	1.0	-1.051	-0.948	-0.865	-0.809

TABLE 3 (CONTD)

$\beta s/\ell = 0.800$

y/s	ξ	C_{p_1}	C_{p_2}	C_{p_3}	C_{p_4}
0.05	0.1	0.664	0.143	0.021	0.003
	0.2	0.411	0.236	0.079	0.022
	0.3	0.223	0.268	0.147	0.065
	0.4	0.044	0.243	0.200	0.125
	0.5	-0.132	0.159	0.212	0.177
	0.6	-0.308	0.017	0.161	0.194
	0.7	-0.484	-0.182	0.020	0.129
	0.8	-0.659	-0.439	-0.234	-0.076
	0.9	-0.834	-0.753	-0.625	-0.493
	1.0	-1.008	-1.125	-1.179	-1.203
0.575	0.6	0.667	0.457	0.270	0.159
	0.7	0.030	0.202	0.200	0.166
	0.8	-0.294	-0.027	0.071	0.106
	0.9	-0.550	-0.308	-0.179	-0.105
	1.0	-0.776	-0.649	-0.581	-0.548

WT.2078.C.P.606.K3 - *Printed in England*

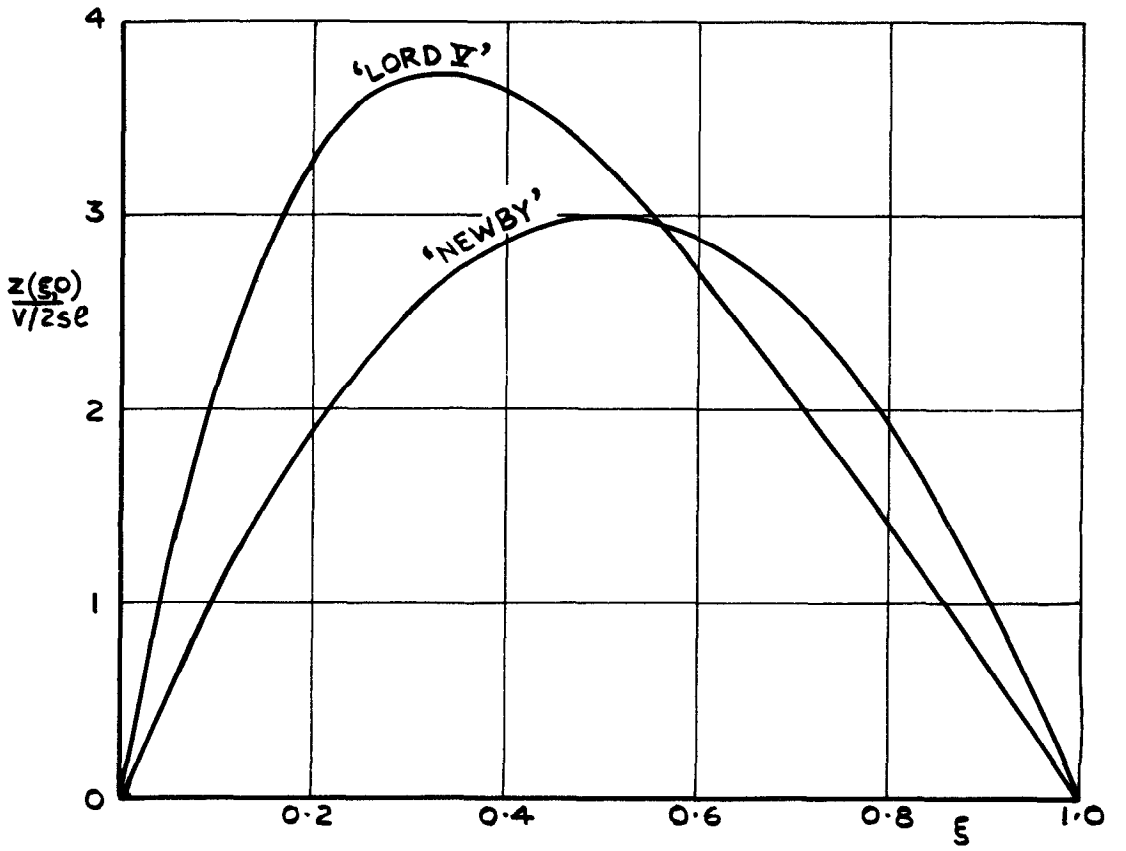

FIG. 1. CENTRE-SECTIONS OF 'LORD V' AND 'NEWBY' WINGS

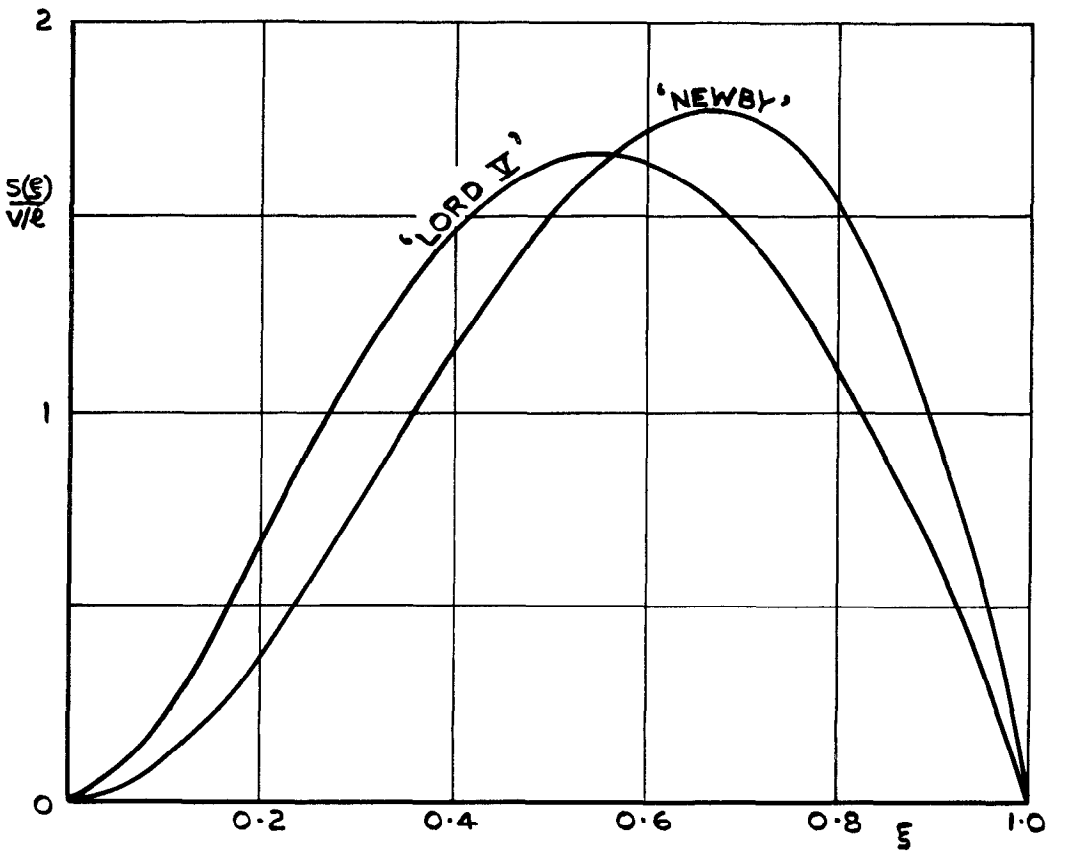

FIG. 2. CROSS-SECTIONAL AREA DISTRIBUTIONS OF 'LORD V' AND 'NEWBY' WINGS.

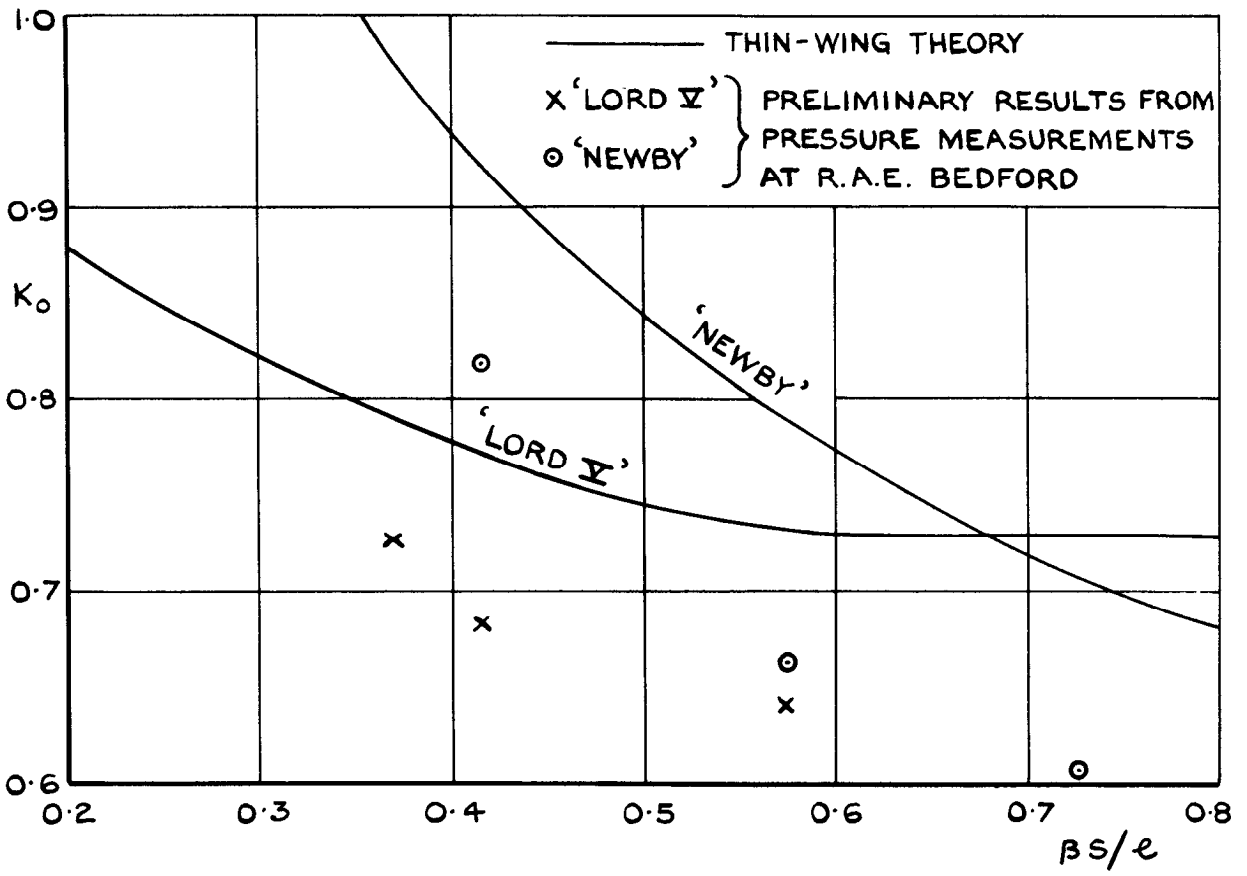

FIG. 3. DRAG FACTOR OF 'LORD V' AND 'NEWBY' WINGS.

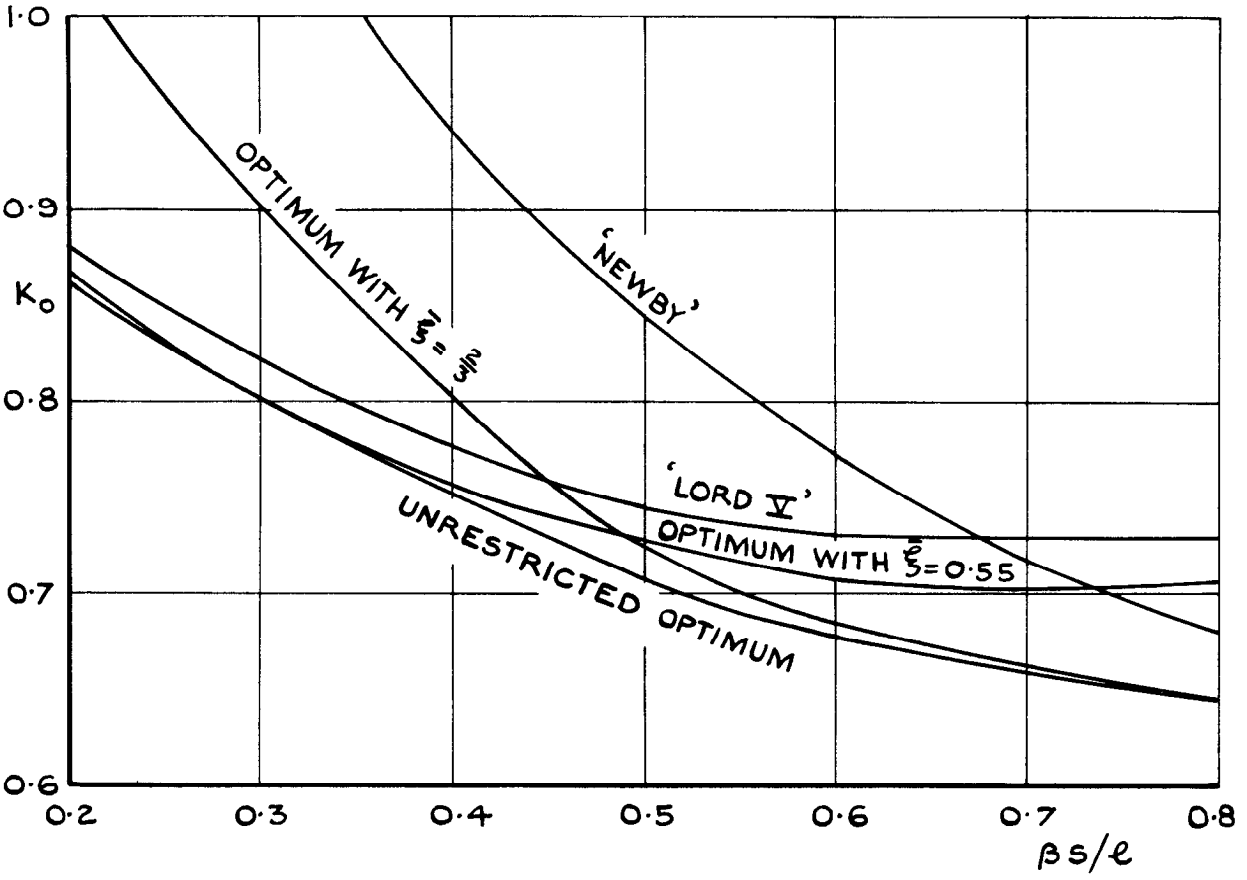

FIG.4. DRAG FACTOR OF WINGS WITH QUINTIC POLYNOMIAL CENTRE-SECTIONS, CALCULATED BY THIN-WING THEORY.

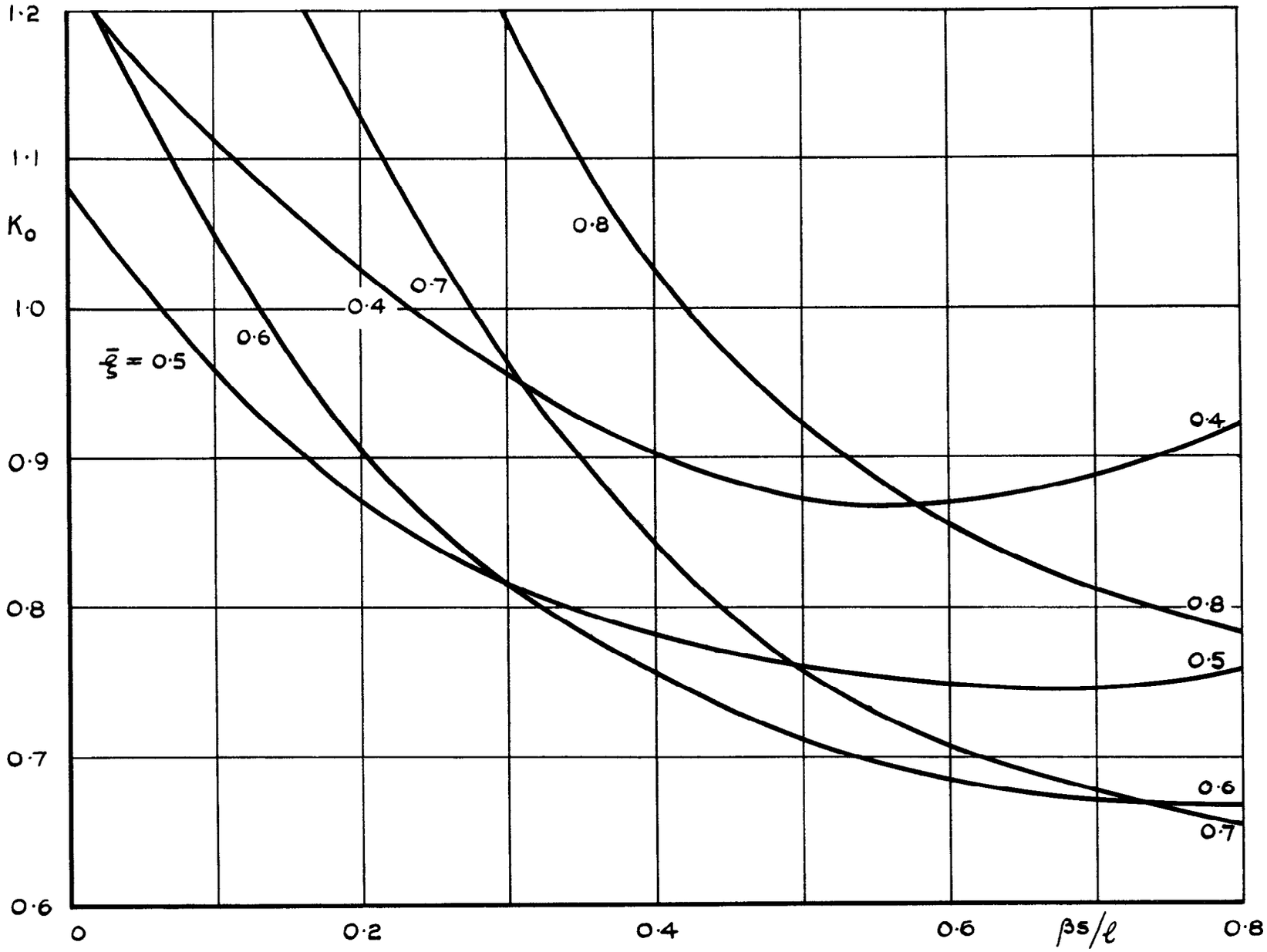

FIG.5. MINIMUM DRAG OF WINGS WITH QUINTIC POLYNOMIAL CENTRE-SECTIONS AND FIXED $\bar{\xi}_s$ (THIN-WING THEORY).

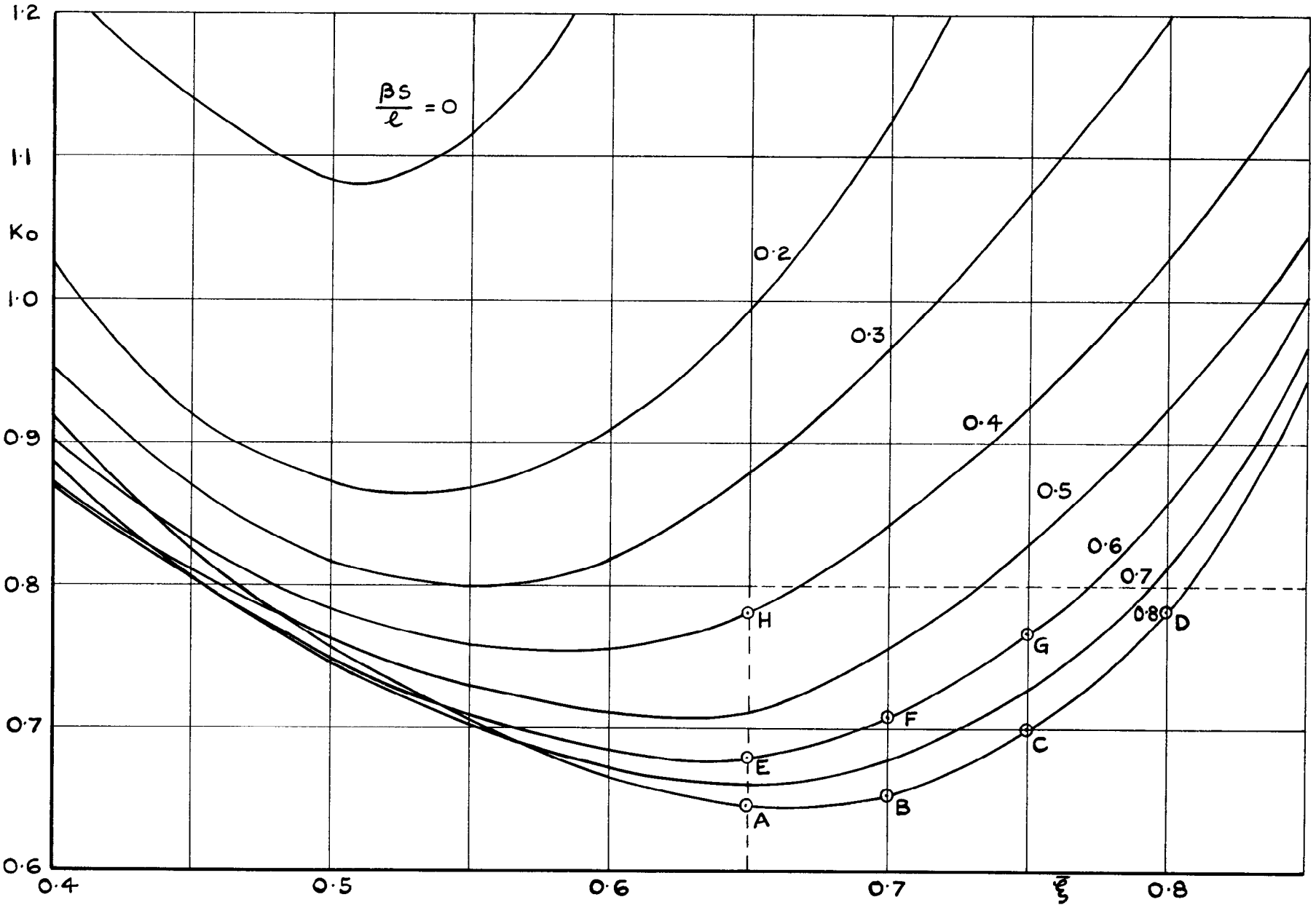

FIG. 6. MINIMUM DRAG OF WINGS WITH QUINTIC POLYNOMIAL CENTRE-SECTIONS AND FIXED $\bar{\xi}$ (THIN-WING THEORY).

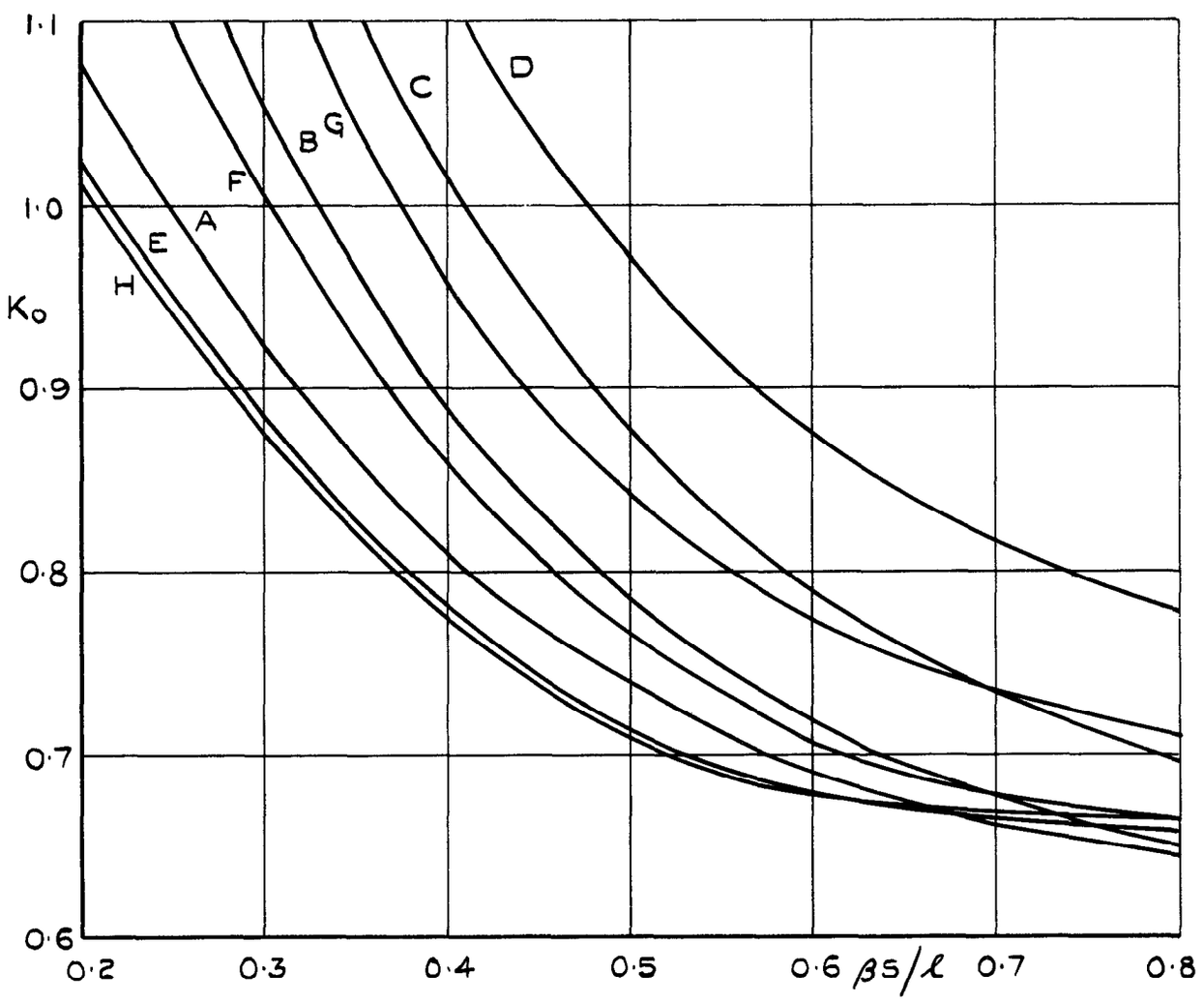

FIG. 7. VARIATION OF DRAG FACTOR WITH MACH NUMBER FOR WINGS A TO H (THIN-WING THEORY)

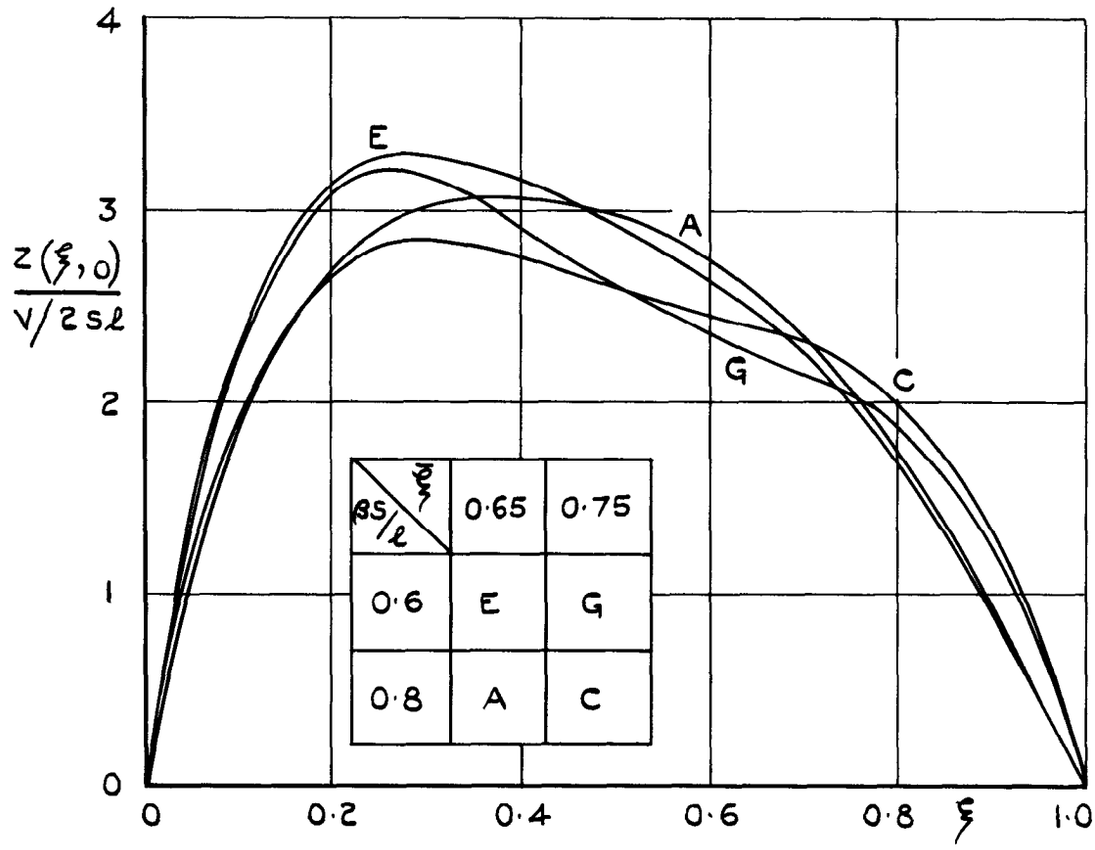

FIG. 8. CENTRE - SECTIONS OF WINGS A,C,E,G DESIGNED FOR VARIOUS $\bar{\xi}$ AND $\beta s/\ell$.

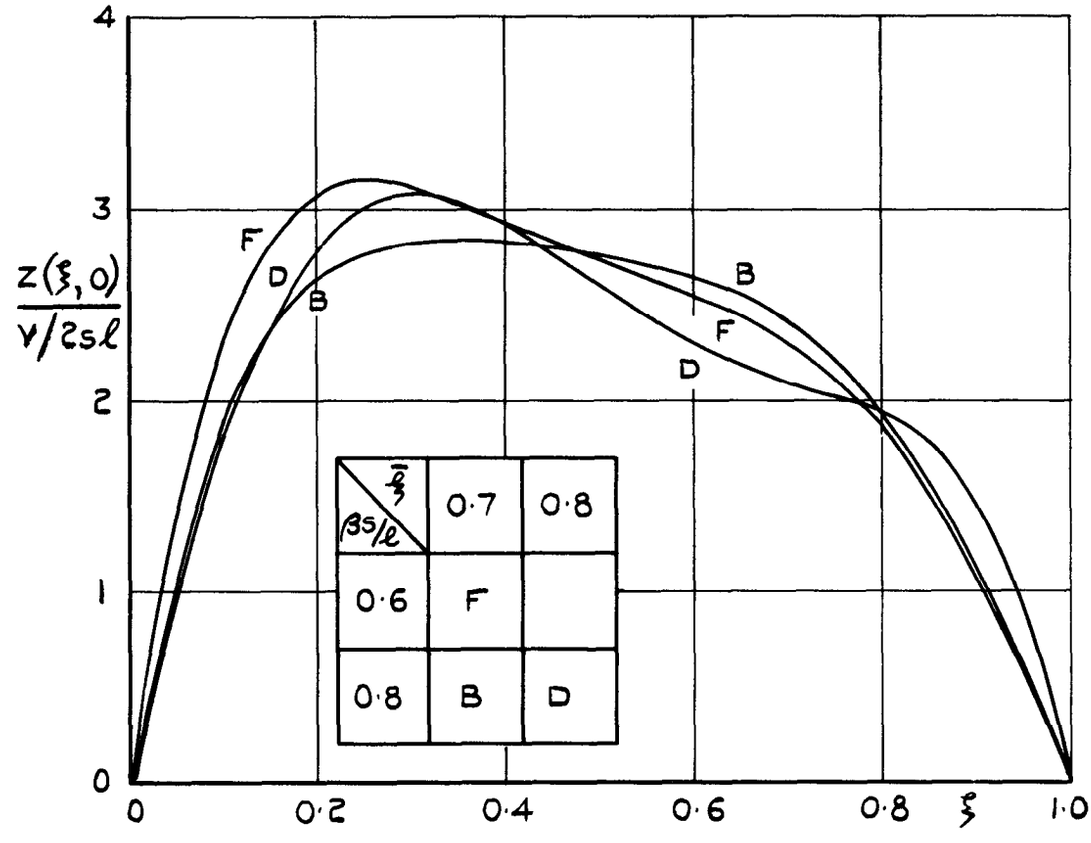

FIG. 9. CENTRE - SECTIONS OF WINGS B,D,F DESIGNED FOR VARIOUS $\bar{\xi}$ AND $\beta s/\ell$.

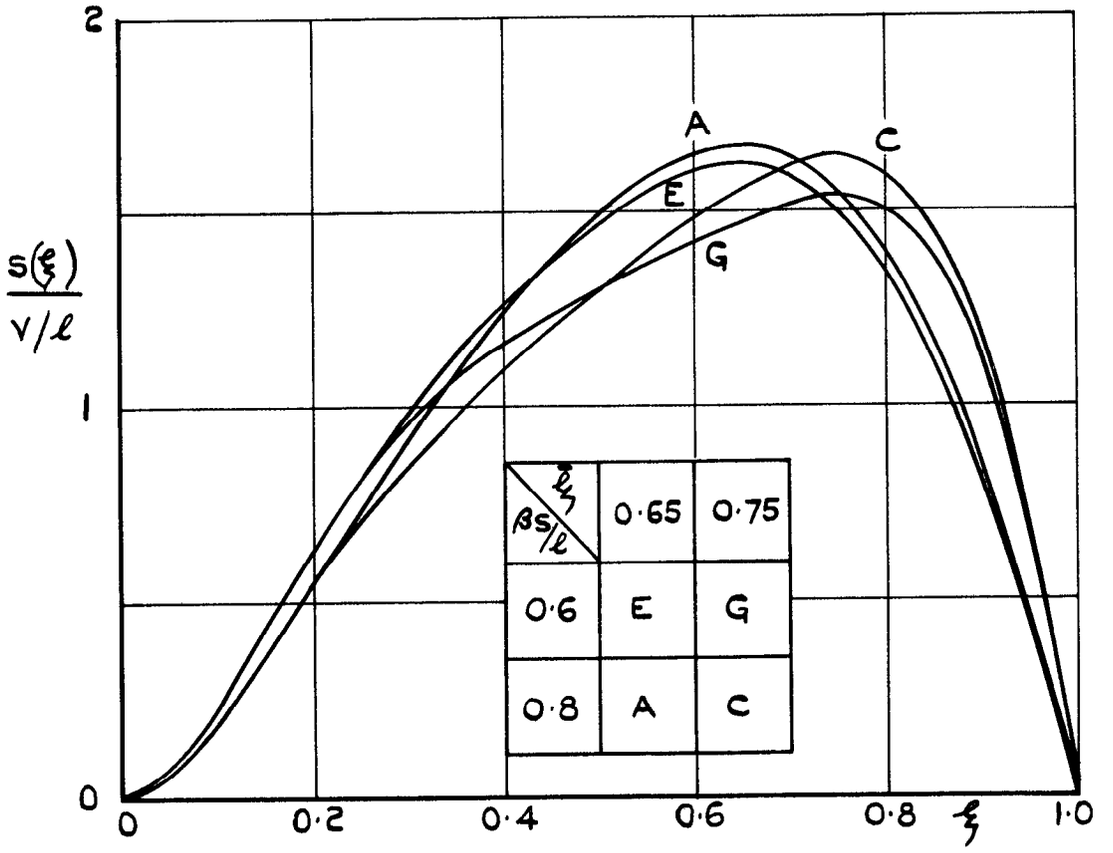

FIG. 10. CROSS - SECTIONAL AREA DISTRIBUTIONS OF WINGS A,C,E,G.

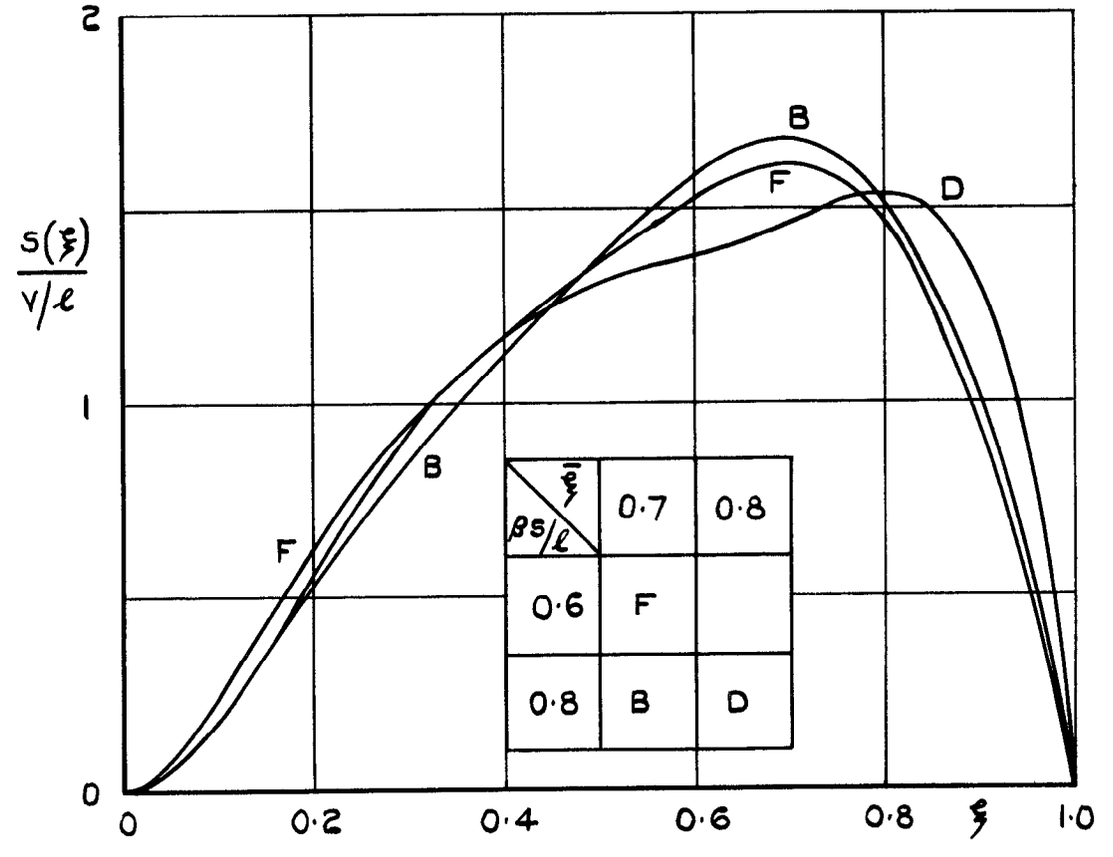

FIG. 11. CROSS - SECTIONAL AREA DISTRIBUTIONS OF WINGS B,D,F.

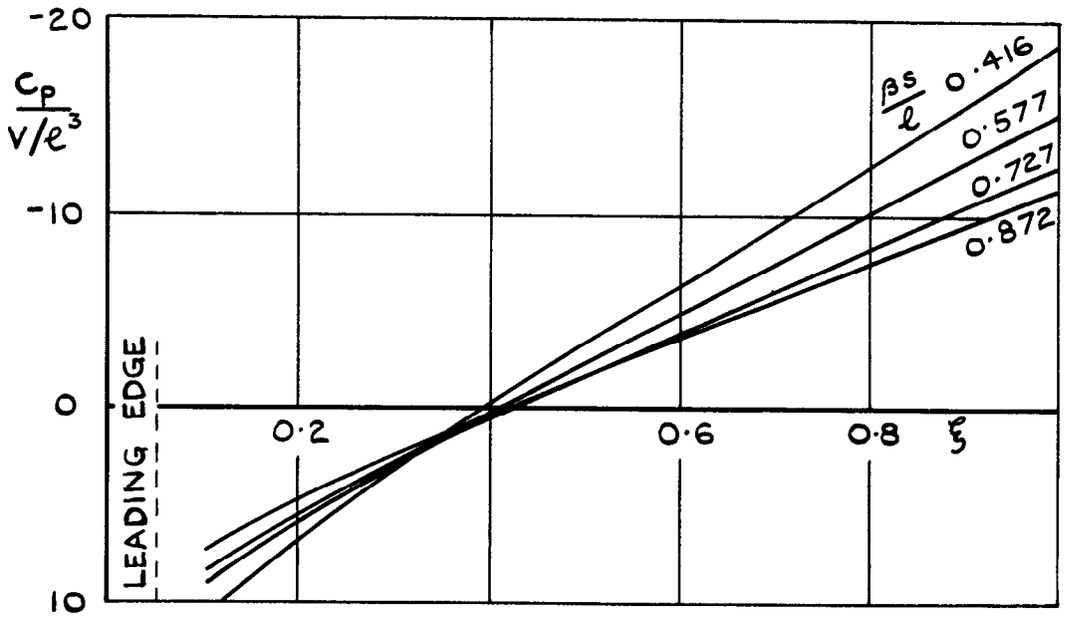

FIG.12. PRESSURE DISTRIBUTIONS AT $y = 0{\cdot}05\,s$ ON 'NEWBY' WING (THIN-WING THEORY).

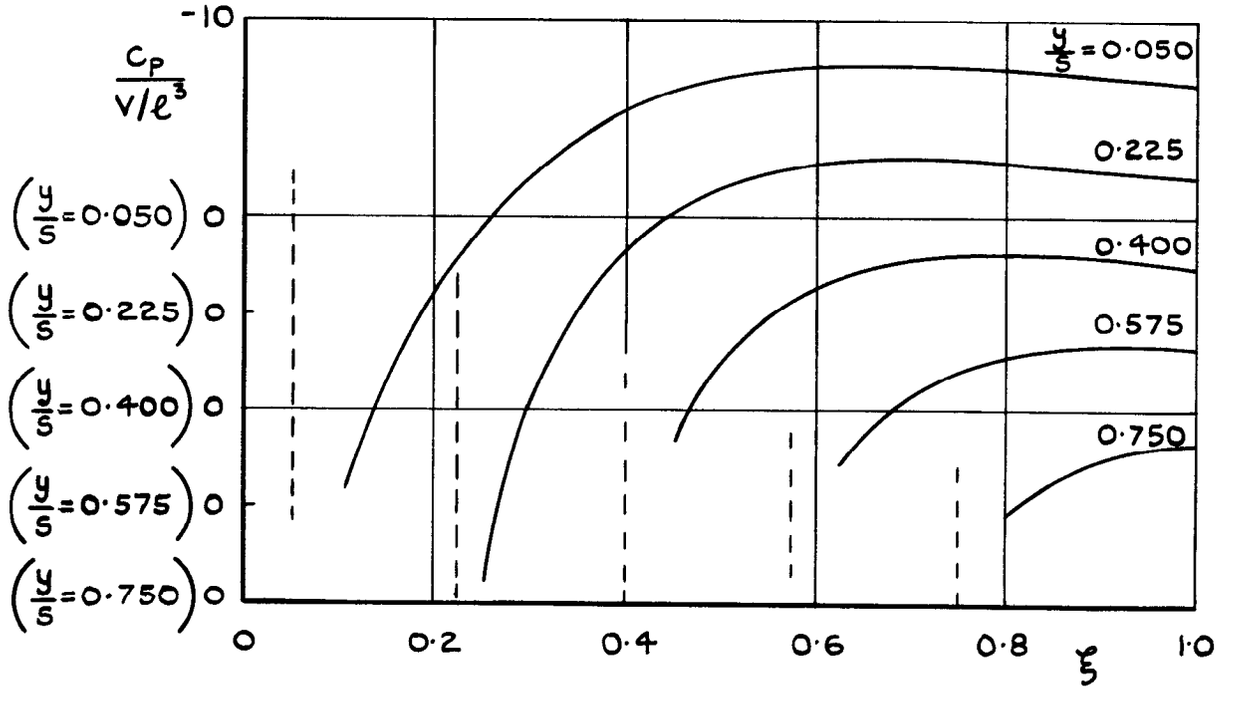

FIG.13. PRESSURE DISTRIBUTION ON 'LORD V' WING, $\beta s/\ell = 0{\cdot}577$ (THIN-WING THEORY).

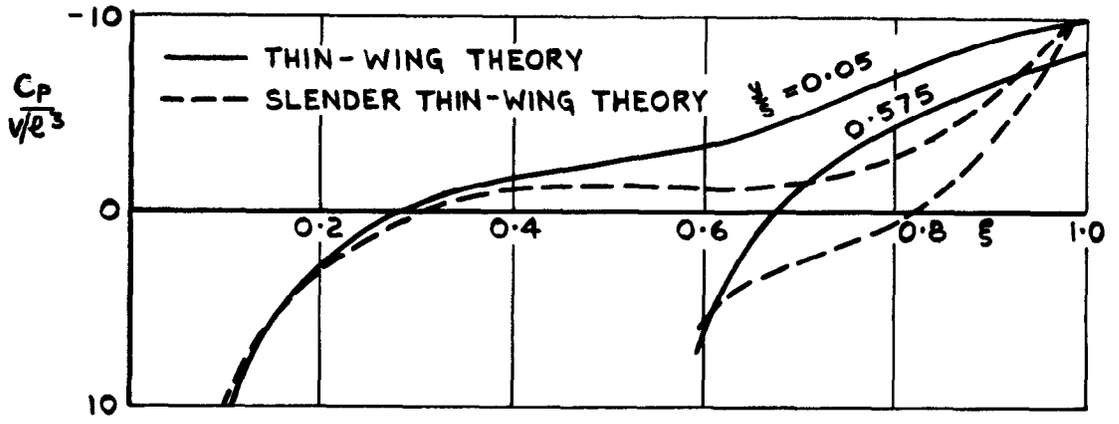

FIG.14(a) PRESSURE DISTRIBUTION ON WING A. $\beta s/\ell = 0{\cdot}8$.

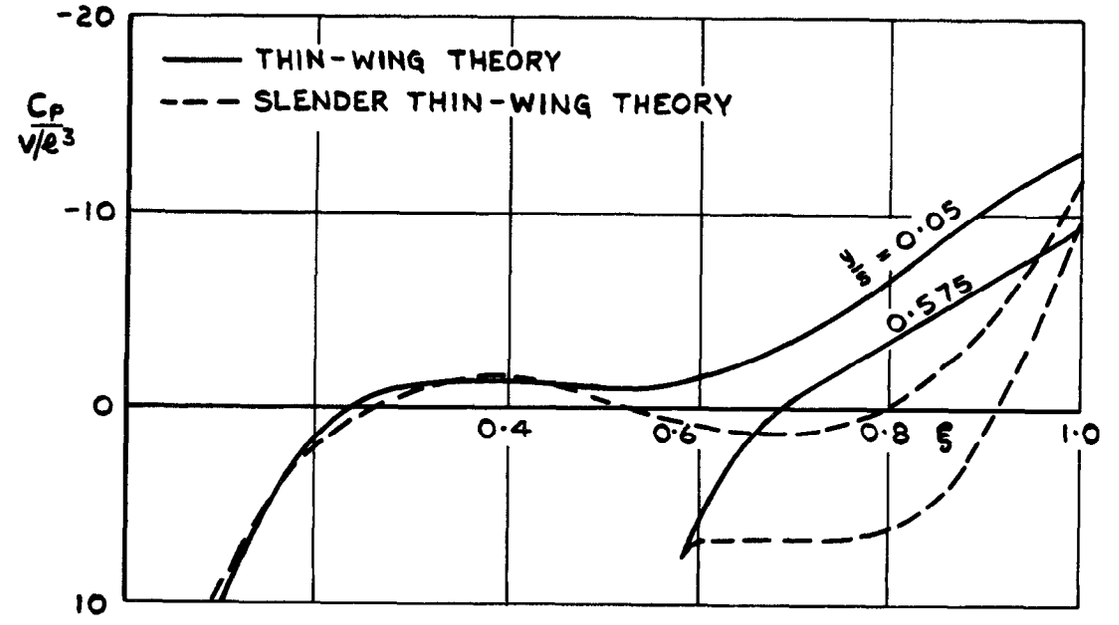

FIG.14 (b). PRESSURE DISTRIBUTION ON WING B. $\beta s/\ell = 0{\cdot}8$.

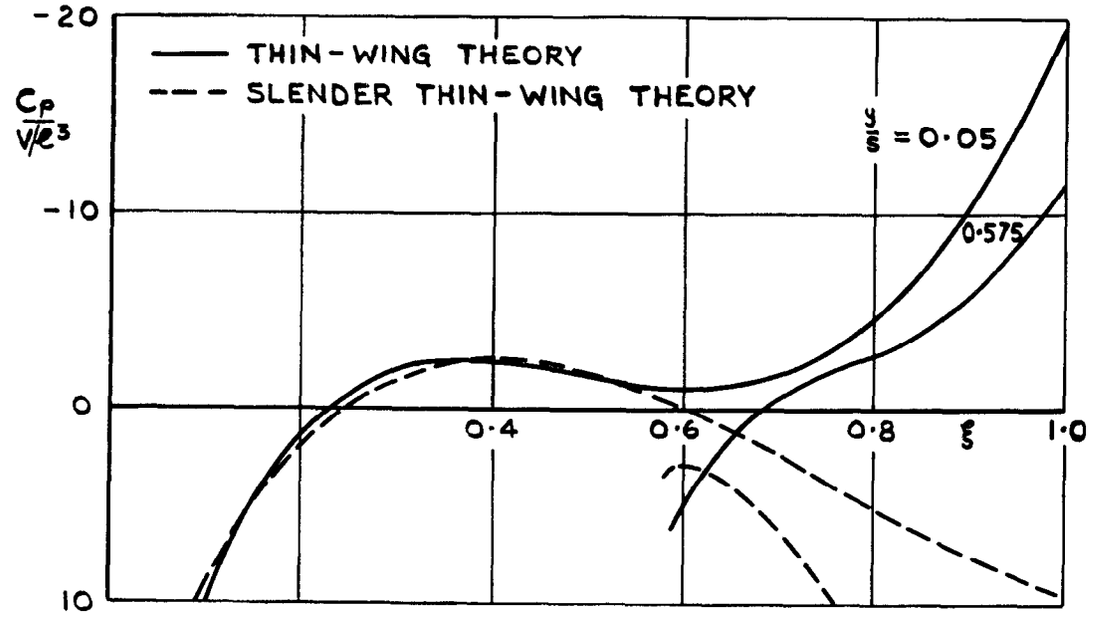

FIG.14 (c). PRESSURE DISTRIBUTION ON WING C. $\beta s/\ell = 0{\cdot}8$.

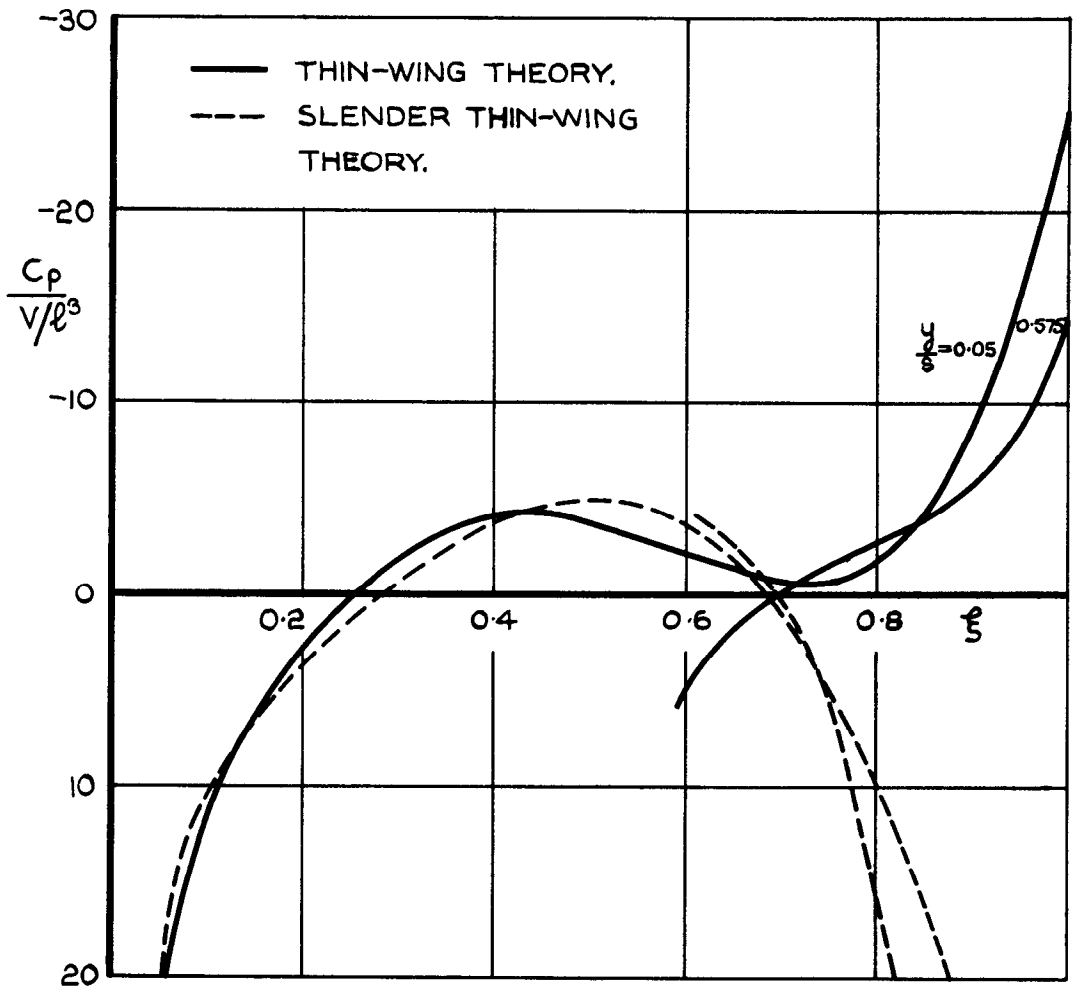

FIG. 14. (d). PRESSURE DISTRIBUTION ON WING D AT $\beta s/\ell = 0·8$.

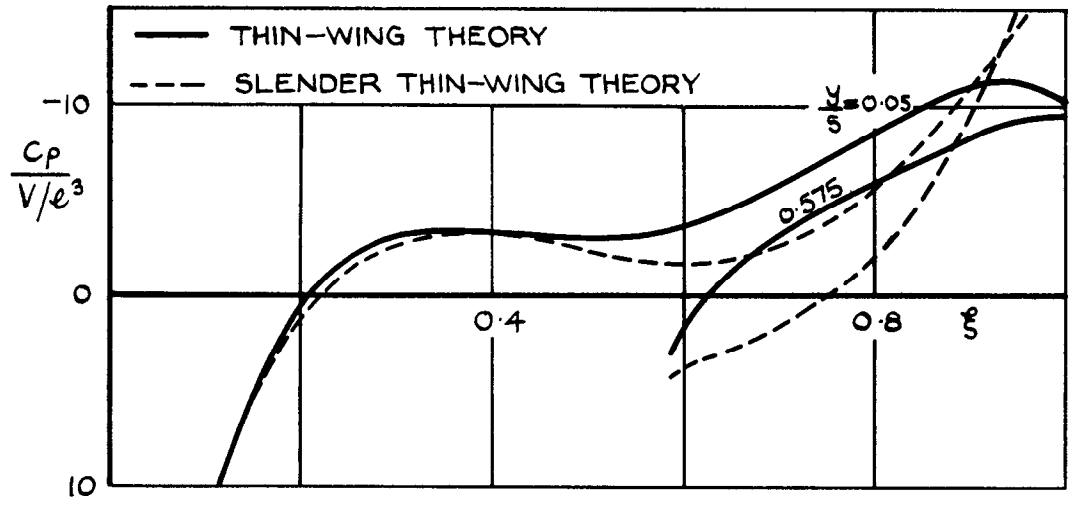

FIG. 14. (e). PRESSURE DISTRIBUTION ON WING E AT $\beta s/\ell = 0·577$.

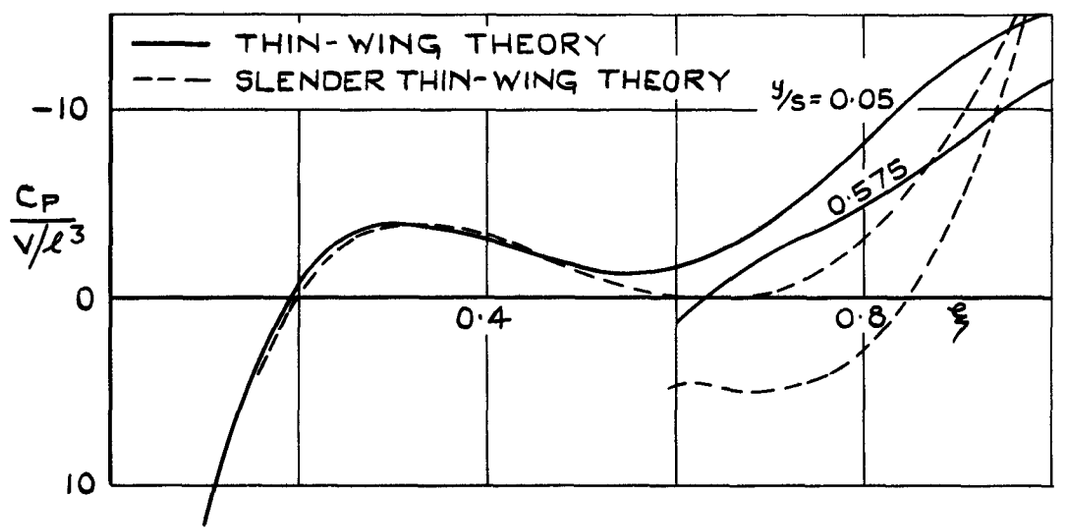

FIG. 14. (f) PRESSURE DISTRIBUTION ON WING F AT $\beta s / \ell = 0.577$.

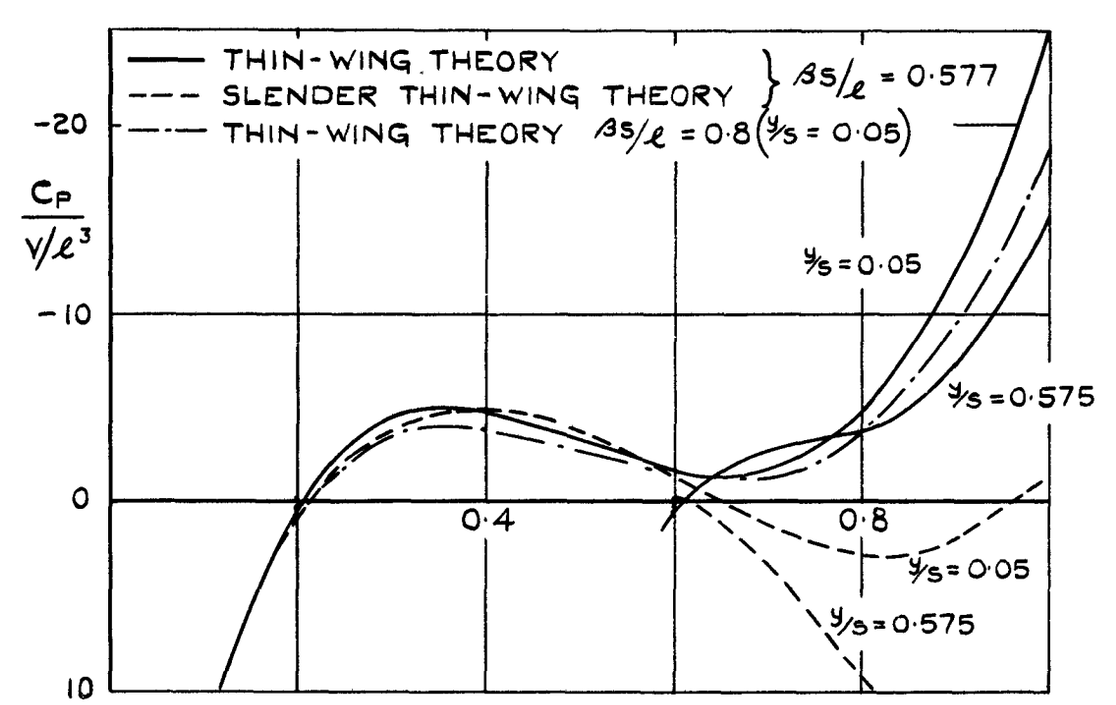

FIG. 14. (g) PRESSURE DISTRIBUTION ON WING G AT $\beta s / \ell = 0.577$ AND 0·8.

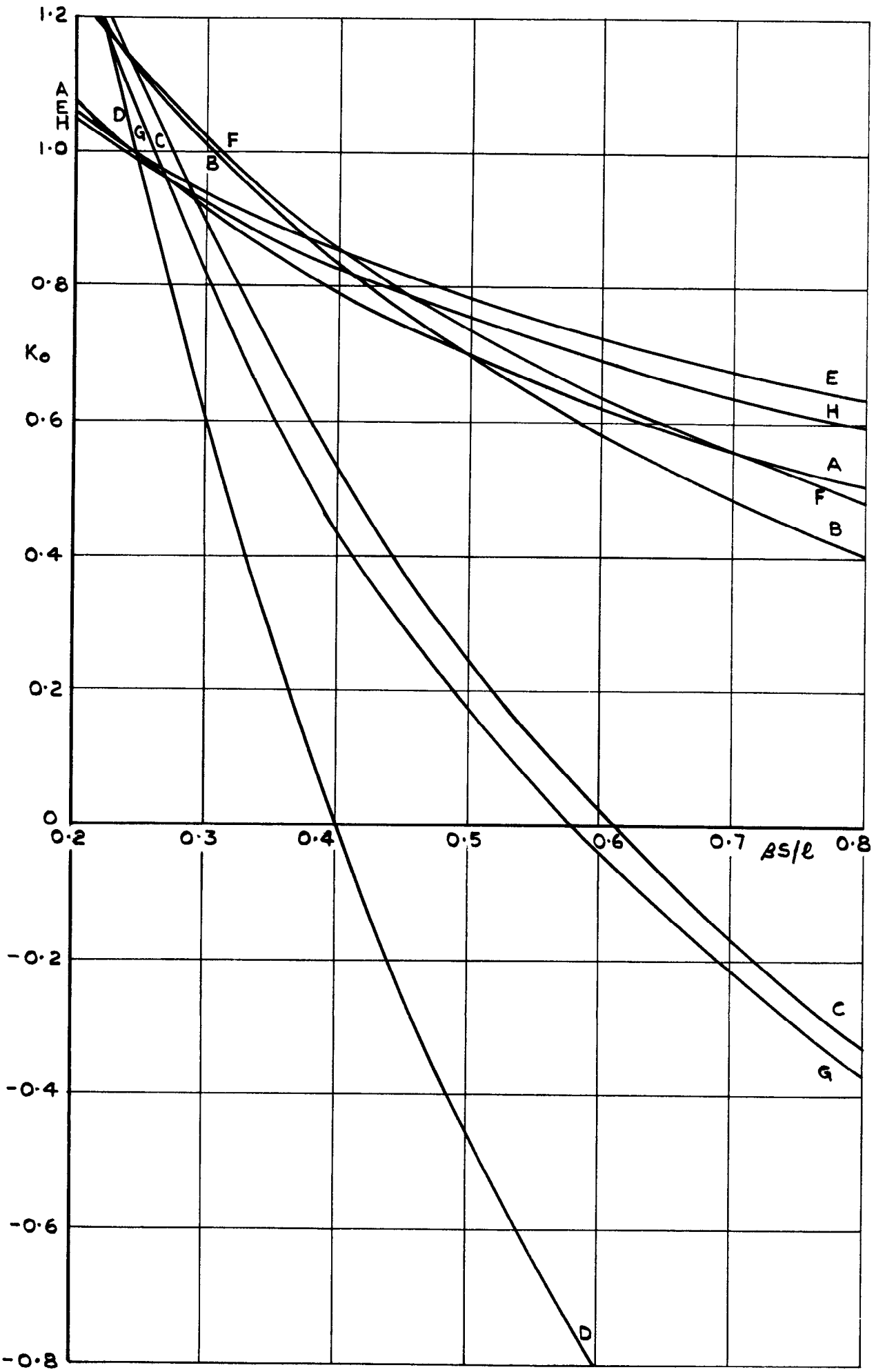

FIG. 15. VARIATION OF DRAG FACTOR WITH MACH NUMBER ACCORDING TO SLENDER-BODY THEORY FOR WINGS A-H.

A.R.C. C.P. No.606

533.693.3 :
533.692.2 :
533.6.013.12 :
533.6.048.2

THE CALCULATED EFFECT OF THE STATION OF MAXIMUM CROSS-SECTIONAL AREA ON THE WAVE DRAG OF DELTA WINGS.
Smith, J.H.B. and Thomson, W. September, 1961.

Use is made of previously calculated properties of a family of delta wings with subsonic leading edges and diamond cross-sections to investigate the effects on the drag and pressure distribution due to volume of variations in the streamwise station at which the cross-sectional area is a maximum. For each station of the maximum cross-sectional area and each value of the aerodynamic slenderness ratio, $\beta s/\ell$, the wing of the family which has least drag for given length and volume is found. As the station of maximum cross-sectional area is moved aft from 65% of the length from the apex, the drag of this optimum wing rises; the rise being steeper for lower values of $\beta s/\ell$. In parallel, adverse pressure gradients and the suction on the wing near the trailing edge both increase so that it becomes less likely that the calculated values will be reproduced in a real flow.

A.R.C. C.P. No.606

533.693.3 :
533.692.2 :
533.6.013.12 :
533.6.048.2

THE CALCULATED EFFECT OF THE STATION OF MAXIMUM CROSS-SECTIONAL AREA ON THE WAVE DRAG OF DELTA WINGS.
Smith, J.H.B. and Thomson, W. September, 1961.

Use is made of previously calculated properties of a family of delta wings with subsonic leading edges and diamond cross-sections to investigate the effects on the drag and pressure distribution due to volume of variations in the streamwise station at which the cross-sectional area is a maximum. For each station of the maximum cross-sectional area and each value of the aerodynamic slenderness ratio, $\beta s/\ell$, the wing of the family which has least drag for given length and volume is found. As the station of maximum cross-sectional area is moved aft from 65% of the length from the apex, the drag of this optimum wing rises; the rise being steeper for lower values of $\beta s/\ell$. In parallel, adverse pressure gradients and the suction on the wing near the trailing edge both increase so that it becomes less likely that the calculated values will be reproduced in a real flow.

A.R.C. C.P. No.606

533.693.3 :
533.692.2 :
533.6.013.12 :
533.6.048.2

THE CALCULATED EFFECT OF THE STATION OF MAXIMUM CROSS-SECTIONAL AREA ON THE WAVE DRAG OF DELTA WINGS.
Smith, J.H.B. and Thomson, W. September, 1961.

Use is made of previously calculated properties of a family of delta wings with subsonic leading edges and diamond cross-sections to investigate the effects on the drag and pressure distribution due to volume of variations in the streamwise station at which the cross-sectional area is a maximum. For each station of the maximum cross-sectional area and each value of the aerodynamic slenderness ratio, $\beta s/\ell$, the wing of the family which has least drag for given length and volume is found. As the station of maximum cross-sectional area is moved aft from 65% of the length from the apex, the drag of this optimum wing rises; the rise being steeper for lower values of $\beta s/\ell$. In parallel, adverse pressure gradients and the suction on the wing near the trailing edge both increase so that it becomes less likely that the calculated values will be reproduced in a real flow.

Published by
HER MAJESTY'S STATIONERY OFFICE

To be purchased from
York House, Kingsway, London w.c.2
423 Oxford Street, London w.1
13A Castle Street, Edinburgh 2
109 St. Mary Street, Cardiff
39 King Street, Manchester 2
50 Fairfax Street, Bristol 1
35 Smallbrook, Ringway, Birmingham 5
80 Chichester Street, Belfast 1
or through any bookseller

Printed in England

S.O. CODE No. 23-9013-6